Improving the performances of current optical interferometers & future designs
Proceedings of Haute Provence Observatory Colloquium (23-27 September 2013)
Edited by L. Arnold, H. Le Coroller & J. Surdej

Nanometer-scale absolute laser ranging: exploiting a two-mode interference signal for high accuracy distance measurements

D.-H. Phung[1], C. Courde[2], C. Alexandre[3], M. Lintz[1]

[1] *ARTEMIS, Univ. de Nice, Observatoire de la Côte d'Azur & CNRS, Bd de l'Observatoire, 06304 Nice, France (corresp. author michel.lintz@oca.eu)*

[2] *Univ. Nice Sophia Antipolis, CNRS, IRD, Observatoire de la Côte d'Azur, Géoazur UMR 7329, 250 rue Albert Einstein - 06560 Valbonne - France*

[3] *CEDRIC-LAETITIA, CNAM, 292 Rue Saint Martin, 75141, Paris cedex 03, France*

Abstract. Absolute distance measurement with accuracy below the micron scale is important in astronomical optical interferometry. We present here an absolute laser rangefinder which relies on the detection of a two mode interference signal. We exploit the specific signature of the signal to extract both the interferometric and synthetic phase measurements, leading to distance measurement with nanometric accuracy. A resolution of 100 pm has been achieved in 75 μs with a relatively simple laser source. Amplitude to phase coupling in the detection chains turns out to be the largest source of systematic errors. A specific detection scheme is implemented, using optical demodulation of the microwave optical signal, to reduce amplitude-to-phase related systematic errors to below the required level.

1. Introduction

Measuring distances is important in many areas of technology. In space geodesy, where formation flight is used for mapping the high harmonics of the earth's gravity field, the measurement of the inter-spacecraft distance variation provides the input for the determination of the gravity field gradients. Astronomical optical interferometry is another domain which requires accurate determination of distances. The phase of the different beams that interfere has to be controlled, to get the required phase condition at recombination (destructive interference in nulling interferometry, constructive interference in imaging techniques, such as diluted telescopes, see Session 6 of this colloquium). Hence absolute distances have to be known to about 1 μm in ground instruments, where atmospheric turbulence limits the achievable phase stability. In space instruments, much better conditions can in principle be achieved, and accuracy of the absolute distance measurement has to reach the nanometer scale.

In the measurement of long distances, multi-wavelength interferometry has been able to provide both long synthetic wavelength and sub-micron accuracy (Salvadé et al. 2008). Using multiple 40 GHz phase modulations of a CW laser beam, MSTAR (Lay et al. 2003) has reached 100 nm scale accuracy. Frequency combs from femtosecond lasers are increasingly used in absolute distance measurement setups, inspired either from optical linear sampling (Coddington et al. 2009), or from dispersive interferometry (van den Berg et al. 2012). A different approach, that has been considered to some extent by Joo, Kim, & Kim (2008), consists in combining
i) a high precision, interferometric optical phase measurement, wrapped in the $[0,\ \lambda_{opt}]$ interval
ii) a carrier modulation phase measurement at frequency ≈ 20 GHz, wrapped in the $[0,\ \Lambda \equiv c/F]$ interval
iii) a time-of-flight measurement of the distance d.

If measurement iii) is accurate enough to bring unambiguous meaning to measurement ii), which in turn has good enough accuracy to give absolute significance to measurement i), then absolute distances can be measured with an accuracy far better than an optical wavelength. It appears, however, that long term (> 1 s) drifts in high frequency measurements exceed the limit $\pi\lambda_{opt}/\Lambda$ beyond which measurement ii) fails to provide unambiguous determination of $2d/\lambda_{opt}$.

In this work we demonstrate that this problem is solved by a measurement scheme in which both phase measurements i) and ii) are obtained, in a consistent way, from the same interference measurement, using the 20 GHz beatnote, two-mode laser beam. The two-mode interferometer signal is exploited in a way such that both the optical phase and the synthetic phase are retrieved, separately, after a procedure that lasts about 100 μs and eliminates long term drifts of the phase and of the gain in microwave detection chains. On a simple set-up on which a ≈ 7.5 m optical path is implemented, we show that this measurement scheme can achieve the conditions required to provide nanometer accuracy absolute distance measurements. Among the systematic effects that show up on the two-mode interference measurements, some are related to the detection chains: cyclic errors and, more importantly, amplitude to phase coupling. The latter appears to be very difficult to correct for at the required precision level, due to thermal processes in the photodetectors. We finally present a way to reduce the AM-to-PM effects by a large factor (1000 in our case) so that AM-to-PM coupling is no longer a problem in our detection scheme. The two-mode interference detection scheme appears to provide a signal capable of nanometer accuracy in long (kilometer scale) distance measurements. A resolution of 130 pm has been achieved over measurements that last about 75 μs, repeated every 135 μs. The $1/\sqrt{N}$ dependence of the resolution, where N is the number of acquisition cycles, is expected to be obtained if the measured path length is not affected by ambient turbulence or acoustic perturbations.

2. Measurement principles

Two narrow-linewidth, single-mode fiber lasers are phase-locked (Fatome et al. 2010, § 5) at a frequency of GHz, to provide a two-mode laser source, of known optical frequencies $[\nu_{opt},\ \nu_{opt} + F]$. The corresponding synthetic wavelength $\Lambda =$

c/F is close to 15 mm. In Fig. 1 below, the two-mode laser beam propagates from BS0 to PhD1 along two different paths: a short reference path, of constant length l, and a variable measurement path of length L. The interference of these two beams provides the signal from which we extract the quantity to be measured, the length difference $\Delta L \equiv L - l$.

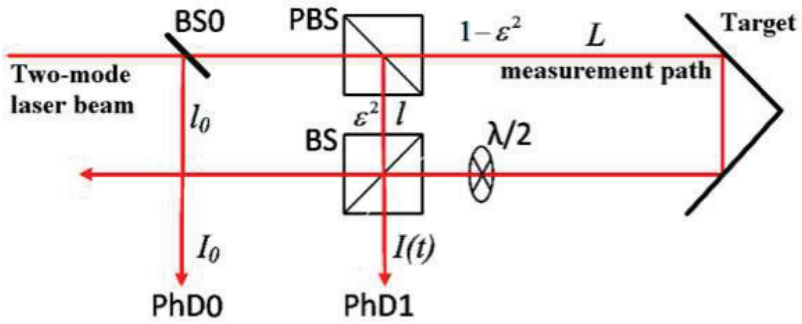

Figure 1.: *Schematic diagram of the telemeter. BS0: beam splitter plate; (P)BS: (polarizing) beam splitter cube.*

The polarization of the initial beam is chosen so that a small fraction of the beam power, $\epsilon^2 =$ a few %, propagates, from PBS to BS, along the reference path, with S polarization. The remaining power (fraction $1-\epsilon^2$) propagates along the measurement path with P polarization (S polarization after the half-wave plate) and interferes with the reference beam. The resulting intensity,

$$\begin{aligned} I(t) = (1-\epsilon^2)\Big[1+\cos\Big(\delta(t-L/c)\Big)\Big] + \epsilon^2\Big[1+\cos\Big(\delta(t-l/c)\Big)\Big] \\ +2\epsilon\sqrt{1-\epsilon^2}\ \cos\Big(\omega(L-l)/c+\delta(L-l)/2c\Big) \\ \times\Big[\cos\Big(\delta(t-(L+l)/2c)\Big)+\cos\Big(\delta(L-l)/2c\Big)\Big], \end{aligned} \tag{1}$$

where $\omega = 2\pi\nu_{opt} = 2\pi c/\lambda_{opt}$ and $\delta = 2\pi F = 2\pi c/\Lambda$, is detected by PhD1. The (reference) photodiode PhD0 delivers a signal whose amplitude and phase are used to eliminate power and phase fluctuations of the laser source. Expression (1) is valid only in vacuum. Application to quantitative measurements in air requires that two indices of refraction, at the two wavelengths, are taken into account.

The measurement exploits the phase Φ and amplitude α of the $\alpha\cos(\delta t - \Phi)$ terms, oscillating at the microwave frequency F. As illustrated in Fig. 2, in which oscillating terms are represented as vectors $\alpha\exp(i\Phi)$ in the complex plane, the measurement signal A is the sum of three terms, $MEAS = (1-\epsilon^2)\exp(i\delta L/c)$, $REF = \epsilon^2\exp(i\delta l/c)$, and the interference contribution:

$$INT = 2\epsilon\sqrt{1-\epsilon^2}\ \cos[(\omega+\delta/2)\Delta L/c] \times \exp\Big(i\delta(L+l)/c\Big). \tag{2}$$

When the optical frequency ν_{opt} of the two-mode source is scanned over more than the free spectral range $FSR \equiv c/\Delta L$, the tip of the vector $A = MEAS + REF + INT$ travels back and forth along the "segment" (Fig. 2-a), of length $4\epsilon\sqrt{1-\epsilon^2}$, characteristic of optical interference. Any deviation from a strictly linear segment reveals the presence of systematic effects.

The dependence on the target position is more complex. Not only the amplitude of the INT vector changes, but its direction, and the $MEAS$ vector direction also change, producing a circular pattern with a large number ($\omega/\delta \approx 10^4$) of spikes. On Fig. 2-b, the choice of $\omega/\delta \approx 20$ allows for the spikes to be conveniently observable. Each spike corresponds to one fringe of the optical interference.

From a *single* measurement of this complex interference signal, one cannot extract the three contributions separately. However, assuming that a time-of-flight measurement has been done beforehand, with a relative accuracy of 10^{-5} or better, one can estimate the free spectral range FSR, and perform *three* measurements $A1, A2, A3$ with an optical frequency of ν_{opt}, $\nu_{opt} + FSR/4$, and $\nu_{opt} + FSR/2$, respectively. Then the three data points of the two-mode interference signal can be processed, in a relatively straightforward manner, to compute, separately, the interferometric phase $\Phi_{inter} \equiv 2\pi\Delta L/\lambda_{opt}$ (mod. 2π) and the synthetic phase $\Phi_{synt} \equiv 2\pi\Delta L/\Lambda$ (mod. 2π). Fast (< 1 μs) change of the optical frequency can be achieved using an acousto-optic modulator (AOM). The accuracy of the measurement relies on the accuracy of the knowledge of ν_{opt} and F.

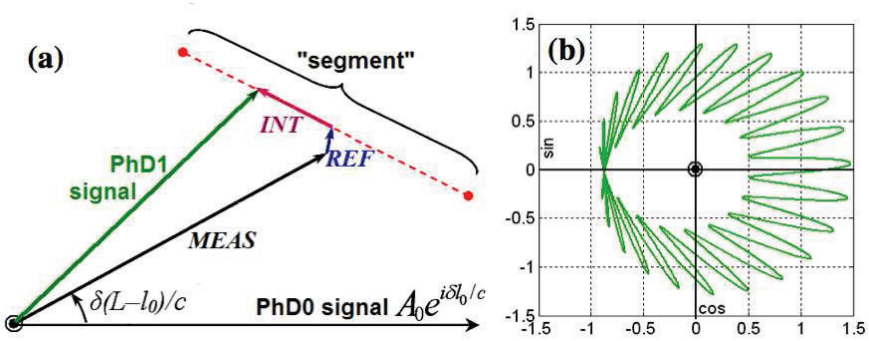

Figure 2.: *Behavior of the two-mode interference signal (PhD1 signal): (a) when the optical frequency of the two-mode source is scanned, (b) when the target moves continuously over one half of the synthetic wavelength, $\Lambda/2$, for $\epsilon = 0.25$. For clarity, Λ/λ_{opt} is chosen equal to 20.*

3. Implementation

In the experimental set-up (Fig. 3) interference takes place at the Glan polarizer which, oriented at 45°, mixes the beams from the reference and measurement arms. Stray contributions to the two-mode interference signal have to be kept below 10^{-4}. Hence, stray beams have to be kept well below 10^{-8}: wedged optics are used to prevent interference due to multiple reflections, which are a significant

source of systematics. The microwave signals (20.04 GHz) are detected by two 20 GHz bandwidth photodiodes, down-converted to 20 MHz by the mixers, and sampled during 10 μs by two 250 MS/s, 14 bit analog-to-digital converters.

The FPGA-based phase meter updates the AOM frequency for the ν_{opt} shifts and calculates the signal amplitudes and phases. Data processing and averaging (Phung 2013) is operated in a way that rejects the slow drifts in the microwave instrumentation, which otherwise would spoil the measurements, adding shifts of ± 1 (or several) times λ_{opt} on the measurement of ΔL. Next section describes phase systematic shifts of thermal origin that have requested a change in the detection setup.

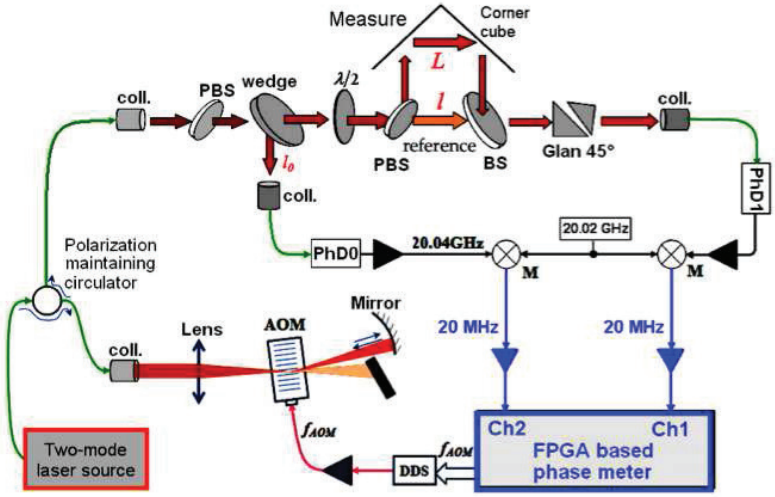

Figure 3.: *Implementation of the range meter. Orange: laser beams; green: optical fiber; black: HF signals; blue: RF signals; coll., fibered collimators; (P)BS: (polarizing) wedged beam splitter plates; Glan 45°: air Glan polarizer; DDS: direct digital synthesizer. M: mixers.*

As shown in Fig. 4, successive elementary measurement cycles, repeated every 130 μs, show the presence of acoustic perturbations, with an amplitude of several nanometers, on the measured length difference. The acoustic perturbations are due to the fans of the electronic equipment in the experimental room, close to the ≈ 7.5 m round trip measurement arm.

The acoustic perturbations of the measurement path will be absent in the measurement of distances in vacuum, and the resolution, about 130 pm over one elementary measurement cycle, is expected to improve with integration time.

4. Amplitude-to-phase (AM-to-PM) effects and their reduction

Systematic errors in the detection chains are of two kinds. The first one is electrical cross-talk, which, if uncorrected for, gives rise to errors of about 10 μm in the ranging measurements. It can be measured, in phase and amplitude, and can

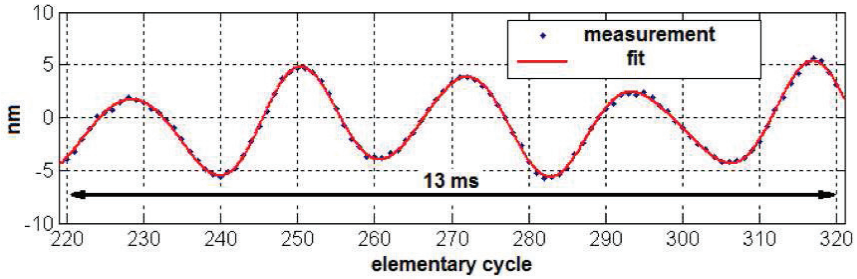

Figure 4.: *One hundred successive length measurements (an offset of* ≈ 7.5 *m is subtracted, for clarity). One point corresponds to one* $A1 \Rightarrow A2 \Rightarrow A3$ *sequence (one "elementary measurement cycle"). The red curve is a fit obtained using 8 harmonic (sine) functions.*

be corrected for, with a good enough accuracy. The second kind of systematics in the detection chain is amplitude-to-phase coupling.

AM-to-PM coupling is well-known in electronics, and has been observed also in high-bandwidth photodiodes. On our set-up, if uncorrected, it gives rise to ranging errors of the order of 100 μm (Phung 2013). One might think that, knowing the amplitude, AM-to-PM coupling related errors can be corrected for, if the phase-vs-amplitude curve is measured beforehand over the range of experimental values. However, this approach fails with ranging signal data, in which the amplitude changes at microsecond time scales, along a complex pattern. This is due to the fact that AM-to-PM coupling has two contributions related to the physics of the photodiode junction. One is the screening of the applied electric field due to the carriers created in the junction (Taylor et al. 2011, Zhang et al. 2012): it develops at picosecond time scales, and can be considered as instantaneous in our measurements. But the large (up to factors of 3) optical power changes also give rise to another type of AM-to-PM coupling during the $A1 \Rightarrow A2 \Rightarrow A3$ sequence. The heating of the photodiode junction under the Joule power $V_{bias} \times I_{photo}$ (Chen et al. 2009) also changes, giving rise to a *transient* AM-to-PM, at time scales that range from microseconds to milliseconds. As the transient are not exactly exponential with time, correction of the phase systematic errors is not perfect. It removes the errors in the ranging measurement by a considerable factor (from 100 μm peak-to-peak to 3 μm, see Fig. 5-a). But on the corrected ranging results, systematic errors are still observable as shifts by $+$ or $-\lambda_{opt}$, which prevent from reaching nanometer scale accuracy.

As suggested by Kim & Kärtner (2010), a modification of the detection setup allows to reduce by a large factor the systematic errors on the phase of the detected signals. It consists in demodulating the 20 GHz signal, not by a microwave mixer (as in Fig. 3), but by an integrated optics intensity modulator placed before the measurement chain photodiode. Then (Phung et al., submitted), the AM-to-PM couplings are expected to be reduced by the ratio of the microwave and intermediate frequencies. On Fig. 5-b, an AM-to-PM coupling is still observable (top graph), but it is attributed to the intermediate frequency

amplifier (right blue triangle on Fig. 3). Numerical correction of this systematic phase error is efficient, and the convergence rate reaches 92% while the expected convergence rate is 93.5% (as no 20 GHz modulator was available, we used a 10 GHz modulator, with low 20 GHz modulation efficiency, leading to a reduced signal-to-noise ratio).

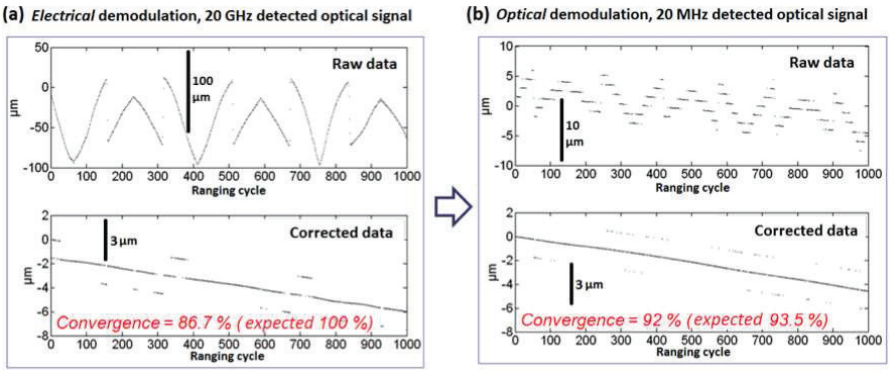

Figure 5.: *Ranging data recorded when the target is slowly moving (2 µm/minute). The retrieved arm length difference ΔL is plotted for successive ranging cycles, with an offset of $\approx$ 7.5 m. (a): the set-up of Fig. 3 is used; in the lower graph the data are corrected for electrical cross- talk and AM-to-PM coupling (instantaneous and transient, 20 µs time constant). (b): detection uses optical demodulation. Due to the low intensity modulation efficiency, noise on the data limits the expected convergence to 93.5%.*

5. Conclusion

A two-mode interference signal is used in high sensitivity absolute distance ranging, after a time of flight measurement has provided a preliminary, coarse estimate of the distance. The two-mode interference signal can be processed in a way that both the synthetic wavelength phase, and the optical interference phase can be retrieved, providing, respectively, micron- and nanometer-scale precision. The processing of the data removes the slow drifts that take place in microwave components, by completing an elementary measurement cycle in about 100 μs. A new length measurement is provided after averaging $\approx$50 ms of data. Large (several times 10^{-3} radian) systematic errors due to amplitude-to-phase coupling in the photodiode are removed by optical (rather than electrical) demodulation of the optical 20 GHz signal. Other systematic errors, related to optical interference (Phung 2013, Chapter 5) are kept under control by using wedged optics to prevent stray beams from interfering with the measurement beam or the reference beam. This high accuracy ranging method, allowing a resolution at the 100 pm scale in about 100 μs, appears to be competitive with other ranging schemes with more sophisticated laser sources.

References

Chen, H., Beling, A., Pan, H., & Campbell, J. C 2009, IEEE Journal of Quantum Electronics 45, 1537

Coddington, I., Swann, W. C., Nenadovic, L., & Newbury, N. R. 2009, Nature Photonics, 3, 351

Fatome, J., Pitois, S., Fortier, C., Kibler, B., Finot, C., Millot, G., Courde, C., Lintz, M., & Samain, E. 2010, Optics Communications, 283, 2425

Joo, K. N., Kim, Y., & Kim, S. W. 2008, Optics Express, 16, 19799

Kim, J., & Kärtner, F. X. 2010, Laser and Photonics reviews, 4, 432

Lay, O. P., Dubovitsky, S., Peters, R. D., Burger, J. P., Ahn, S.-W., Steier, W. H., Fetterman, H. R., & Chang, Y. 2008, Optics Letters, 28, 890

Phung, D.-H., Alexandre, C., & Lintz, M., 2013, Optics Letters, 38, 281

Phung, D.-H. 2013, Thèse de doctorat de l'Université de Nice, `http://tel.archives-ouvertes.fr/docs/00/86/80/28/PDF/2013NICE4038.pdf`

Phung, D.-H., Merzougui, M., Alexandre, C., & Lintz M., submitted

Salvadé, Y., Schuhler, N., Lévêque S., & Le Floch S. 2008, Applied Optics, 47, 2715

Taylor, J. et al. 2011, IEEE Photonics Journal, 3, 140

van den Berg, S. A., Persijn, S. T., Kok, G. J. P., Zeitouny, M. G., Bhattacharya, N. 2012, Physical Review Letters, 108, 183901

Zhang, W., Li, T., Lours, M., Seidelin, S., Santarelli, G., & Le Coq, Y. 2012, Applied Physics B, 106, 301